RESEARCH ARTICLE

WILEY

Breakdown of the affective-cognitive network in functional dystonia

Elisa Canu PhD[1] | Federica Agosta MD, PhD[1,4] | Aleksandra Tomic MD, PhD[5] | Elisabetta Sarasso BSc[1,4] | Igor Petrovic MD, PhD[5] | Noemi Piramide BSc[1,4] | Marina Svetel MD, PhD[5] | Alberto Inuggi PhD[6] | Natasa D. Miskovic MD, PhD[5] | Vladimir S. Kostic MD, PhD[5] | Massimo Filippi MD[1,2,3,4] (iD)

[1]Neuroimaging Research Unit, Institute of Experimental Neurology, Division of Neuroscience, Milan, Italy

[2]Neurology Unit, IRCCS San Raffaele Scientific Institute, Milan, Italy

[3]Neurophysiology Unit, IRCCS San Raffaele Scientific Institute, Milan, Italy

[4]Vita-Salute San Raffaele University, Milan, Italy

[5]Clinic of Neurology, Faculty of Medicine, University of Belgrade, Belgrade, Serbia

[6]Unit of Robotics, Brain and Cognitive Sciences, Istituto Italiano di Tecnologia, Genoa, Italy

Correspondence
Massimo Filippi, Neuroimaging Research Unit, Division of Neuroscience, Institute of Experimental Neurology, San Raffaele Scientific Institute, Vita-Salute San Raffaele University, Via Olgettina, 60, 20132 Milan, Italy.
Email: filippi.massimo@hsr.it

Funding information
Ministarstvo Prosvete, Nauke i Tehnološkog Razvoja, Grant/Award Number: Grant #175090

Abstract

Previous studies suggested that brain regions subtending affective-cognitive processes can be implicated in the pathophysiology of functional dystonia (FD). In this study, the role of the affective-cognitive network was explored in two phenotypes of FD: fixed (FixFD) and mobile dystonia (MobFD). We hypothesized that each of these phenotypes would show peculiar functional connectivity (FC) alterations in line with their divergent disease clinical expressions. Resting state fMRI (RS-fMRI) was obtained in 40 FD patients (12 FixFD; 28 MobFD) and 43 controls (14 young FixFD-age-matched [yHC]; 29 old MobFD-age-matched [oHC]). FC of brain regions of interest, known to be involved in affective-cognitive processes, and independent component analysis of RS-fMRI data to explore brain networks were employed. Compared to HC, all FD patients showed reduced FC between the majority of affective-cognitive seeds of interest and the fronto-subcortical and limbic circuits; enhanced FC between the right affective-cognitive part of the cerebellum and the bilateral associative parietal cortex; enhanced FC of the bilateral amygdala with the subcortical and posterior cortical brain regions; and altered FC between the left medial dorsal nucleus and the sensorimotor and associative brain regions (enhanced in MobFD and reduced in FixFD). Compared with yHC and MobFD patients, FixFD patients had an extensive pattern of reduced FC within the cerebellar network, and between the majority of affective-cognitive seeds of interest and the sensorimotor and high-order function ("cognitive") areas with a unique involvement of dorsal anterior cingulate cortex connectivity. Brain FC within the affective-cognitive network is altered in FD and presented specific features associated with each FD phenotype, suggesting an interaction between brain connectivity and clinical expression of the disease.

KEYWORDS

affective-cognitive network, brain functional connectivity, fMRI, functional dystonia, resting state fMRI

1 | INTRODUCTION

Within the functional (psychogenic) neurological disease spectrum, functional movement disorders (FMD) are characterized by motor disturbances not due to a known general medical or neurologic cause (Edwards, Fotopoulou, & Parees, 2013). Despite the number of clinical and neuroimaging studies in the field, the key cerebral areas involved in FMD and their role in patient symptoms still need to be determined.

Several mechanisms are under current interest in FMD and disruption at multiple motor and affective-cognitive levels has been proposed (Perez, Barsky, Daffner, & Silbersweig, 2012): (a) motor inhibition due to dysfunction of primary motor and somatosensory cortices (Cojan, Waber, Carruzzo, & Vuilleumier, 2009); (b) modifications of intentional abilities and motor-planning with abnormal functioning of prefrontal cortex (PFC; de Lange, Toni, & Roelofs, 2010); (c) impaired sustained attention associated with anterior cingulate cortex (ACC) involvement, with the dorsal part often affected in FMD and further related to motor preparation, selection of action, and cognitive control (Boeckle, Liegl, Jank, & Pieh, 2016; Botvinick, Nystrom, Fissell, Carter, & Cohen, 1999; Perez et al., 2012; Perez et al., 2015); (d) altered action authorship perception due to a main dysfunction of the right temporoparietal junction (rTPJ), which is a key brain structure for the sense of "involuntariness" and agency (Edwards et al., 2013; Schrag et al., 2013); and (e) altered self-referential processing, memory retrieval, emotional regulation and awareness subtended by a complex limbic system disconnection (Boeckle et al., 2016; Perez et al., 2015) with a central abnormal recruitment of ventromedial PFC (vmPFC) together with its projections to the "limbic" subcomponents of thalamus (i.e., mediodorsal nucleus [MDN]; Vertes, Linley, & Hoover, 2015), amygdala, and cerebellum (Crus I and II; Stoodley & Schmahmann, 2010).

Functional dystonia (FD) is the most challenging FMD for both diagnosis and treatment (Espay & Lang, 2015). While organic dystonia is primarily considered as a network disorder at cortico-thalamic-basal ganglia level (Lehericy, Tijssen, Vidailhet, Kaji, & Meunier, 2013), FD can be conceptualized as a dysfunction of both motor and affective-cognitive controlling neurocircuits (Mehta, Rowe, & Schrag, 2013). Up to date, only few studies investigated the brain functional abnormalities in FD. Using positron emission tomography of regional cerebral blood flow, Schrag and colleagues observed that, when compared to each other across all the proposed tasks (rest, fixed posturing of the right leg, and during ankle movements), patients with organic dystonia were characterized by a predominant enhanced cerebral blood flow in the primary motor cortex, while FD cases showed a main increase in the cerebellum (Schrag et al., 2013). However, in the movement task compared with the rest condition, the two groups of patients showed a common increased cerebral blood flow in the right dorsolateral PFC (Schrag et al., 2013). These data suggest similar prefrontal alterations during movement in the two forms of dystonia, likely reflecting a common impairment in motor high-order functions despite a different cortical and subcortical engagement. In line with these findings, a recent functional magnetic resonance (fMRI) study comparing FD and organic dystonia cases showed no group differences in activation in response to a pure motor (finger-tapping) task, but a specific decreased activation in FD patients in response to basic and intense emotional stimuli in selected motor, limbic and sensory areas (Espay et al., 2018).

The picture is even more complex as different FD clinical presentations have been recently described. Patients with the typical FD clinical phenotype present fixed dystonia (FixFD), which is characterized by symptom onset in mid-thirties, early fixed abnormal posture mainly affecting extremities, pain at dystonia localization, often with complex regional pain syndrome (CRPS), static or progressive course with spreading of dystonia to other body regions, and no botulinum toxin treatment response (Schrag, Trimble, Quinn, & Bhatia, 2004). In addition, we frequently observed another manifestation of FD that we named "mobile" FD (MobFD) (Petrovic, Tomic, Voncina, Pesic, & Kostic, 2018), characterized by cranial, cervical or trunkal localization, variable intensity of dystonia with phasic characteristics, relapse-remitting course, good response to botulinum toxin treatment, and potential presence of additional FMD or functional neurological disorders. In a recent work (Tomic et al., 2018), we demonstrated that MobFD had structural brain changes in cortical and subcortical gray matter (GM) regions implicated in sensorimotor processing, and emotional and cognitive control. On the other hand, we found that FixFD patients had a massive and distributed white matter (WM) damage in tracts connecting crucial nodes of motor and emotional control circuits but no GM alterations (Tomic et al., 2018).

In line with the hypothesis that the affective-cognitive brain regions might be implicated in the pathophysiology of FD, the aim of the present study was to explore the resting state functional connectivity (FC) of such network in patients with FD, both in FixFD and MobFD cases, relative to healthy controls (HC) and each other. One advantage of resting state fMRI relative to task-based fMRI is that it is not dependent on differential task performance, which is of particular concern when studying clinically heterogeneous diseases like FD. The affective-cognitive network was defined using a seed-based FC analysis, where we arbitrarily focused on some of the brain regions, beyond the basal ganglia, which have been previously observed to be associated with intentional abilities and motor-planning, motor preparation, selection of action and cognitive control, sense of agency, and emotional regulation. We hypothesized that all patients with FD will share common aberrant FC when compared with controls within the prefrontal circuits and their striatal connections. Furthermore, we hypothesized that each clinical phenotype (FixFD and MobFD) would show peculiar alterations in line with their divergent disease clinical expressions (Petrovic et al., 2018). Specifically, compared to MobFD cases, the FixFD group, neurologically more severe and complex form of FD, would show a more severe pattern of aberrant connectivity, which would involve cortical, subcortical, and cerebellar brain regions. In order to test the hypothesis of network-specificity in FD, we also performed an independent component analysis of resting state fMRI data to assess FC in brain networks other than the affective-cognitive one, such as the default mode, visual associative, sensorimotor, cerebellar, executive control, dorsal attention, and salience networks.

TABLE 1 Demographic and clinical features of FD patients and healthy controls

	FixFD	yHC	p FixFD versus yHC	MobFD	oHC	p MobFD versus oHC	p FixFD versus MobFD
N	12	14		28	29		
Age [years]	35.9 ± 15.8	39.8 ± 11.6	0.47	48.9 ± 10.9	52.0 ± 10.7	0.27	0.005
Women/men (% women)	8/4 (67%)	10/4 (71%)	1.00	23/5 (82%)	24/5 (83%)	1.00	0.28
Education [years]	11.1 ± 1.5	14.5 ± 1.9	<0.001	11.3 ± 1.9	13.7 ± 3.0	0.003	0.78
Clinical features							
Age at onset [years]	32.3 ± 15.3			44.3 ± 9.4			0.004
Disease duration [years]	3.4 ± 3.0			4.7 ± 4.6			0.37
Trigger for dystonia [%]	67			61			0.72
Pain in dystonic region [%]	100			54			0.004
CPRS [%]	58			0			<0.001
Sensory trick [%]	0			4			0.51
Botulin toxin [%]	58			64			0.56
Benefit from botulin toxin [%]	10.0 ± 14.1			49.5 ± 24.8			0.001
Specific treatment (dopaminomimetics, anticholinergics, baclofen) [%]	75			11			<0.001
Psychoactive treatment (benzodiazepines, antidepressants) [%]	75			93			0.15
UDRS	14.0 ± 7.9			8.2 ± 5.2			0.01
BFMS, total	19.9 ± 8.5			6.7 ± 4.5			<0.001
BFMS, disability	6.4 ± 5.1			1.6 ± 1.7			<0.001
PMD, total	20.5 ± 5.1			19.1 ± 7.2			0.55
PMD, total phenomenology	12.1 ± 3.7			11.9 ± 5.6			0.90
PMD, total functional	8.4 ± 3.2			7.0 ± 3.6			0.26
Global cognition							
MMSE	28.7 ± 1.8	30.0 ± 0.0	0.02	28.0 ± 1.6	29.9 ± 0.3	<0.001	0.23
Psychiatric features							
HAMD	13.1 ± 10.8			17.7 ± 10.2			0.29
HAMA	9.3 ± 9.0			13.5 ± 10.1			0.24
Apathy scale	13.5 ± 11.0			19.3 ± 11.2			0.16
DES-II	5.2 ± 7.7			4.2 ± 6.7			0.69
SDQ-20	31.7 ± 10.3			27.8 ± 9.8			0.28

Note: Values denote means ± *SD*s or percentage for continuous and categorial variables, respectively. *p* values refer to ANOVA models (false discovery rate corrected for multiple comparisons), followed by post hoc pairwise comparisons or Fisher's exact test.

Abbreviations: BFMS, Burke Fahn Marsden Scale; CPRS, Complex Pain Regional Syndrome; DES, Dissociative Experience Scale; FixFD, fixed functional dystonia; HAMA, Hamilton Anxiety Rating Scale; HAMD, Hamilton Depression Rating Scale; yHC, young healthy controls; yrs, years; MMSE, Mini Mental State Examination; MobFD, mobile functional dystonia; oHC, old healthy controls; PMD, Psychogenic Movement Disorder; SDQ, Somatoform Disorders Questionnaire; UDRS, Unified Dystonia Rating Scale.

2 | METHODS

2.1 | Participants

In this cross-sectional study, we included 40 patients with FD that fulfilled criteria of "clinically documented" FMD (Gupta & Lang, 2009). All patients included in the present study were part of a previous work on structural brain changes in FD (Tomic et al., 2018). Standard investigations for secondary dystonia (Calne & Lang, 1988) were normal in all

patients, including brain routine MRI. Genetic tests for mutations in the DYT1, DYT6, and DYT11 genes were negative in all patients. FD patients were further subdivided into two groups, according to our previous proposal (Petrovic et al., 2018): FixFD (N = 12) and MobFD (N = 28). Each FD group was matched by age and sex with a group of healthy controls (HC): (a) younger healthy controls (yHC, N = 14) were matched with FixFD group and (b) older healthy controls (oHC, N = 29) were matched with MobFD group (Table 1). All participants were excluded if they had: medical illnesses or substance abuse that could interfere with cognitive

functioning; any (other) major systemic or neurological illnesses and other causes of focal or diffuse brain damage at routine MRI.

All patients were examined by experienced movement disorders specialists (Table 1). The disease severity was assessed by the Unified Dystonia Rating Scale (UDRS) (Comella et al., 2003), Burke–Fahn–Marsden Dystonia Rating Scale (BFMRS) (Burke et al., 1985), and the Psychogenic Movement Disorders Scale (PMDS) (Hinson, Cubo, Comella, Goetz, & Leurgans, 2005). All participants underwent psychiatric examination and interview according to DSM-V criteria as part of diagnostic procedure. Psychiatric evaluation assessed mood and motivation with Hamilton Depression Rating Scale (HAMD) (Hamilton, 1960), Hamilton Anxiety Rating Scale (HAMA) (Hamilton, 1959), Apathy Scale (Marin, Biedrzycki, & Firinciogullari, 1991), and dissociative symptoms with Somatoform Dissociation Questionnaire (SDQ-20) (Nijenhuis, Spinhoven, Van Dyck, Van der Hart, & Vanderlinden, 1996) and Dissociative Experiences Scale II (DES-II; Carlson et al., 1993). All participants were examined with the Mini-Mental State Examination (MMSE; Folstein, Folstein, & McHugh, 1975) in order to assess global cognition. Botulinum toxin treatment response was defined as self-rated clinical improvement in percentage (Table 1).

Local ethical standards committee on human experimentation approved the study protocol and all participants provided written informed consent prior to study inclusion.

2.2 | MRI acquisition

MRI scans were obtained on a 1.5 Tesla Philips Medical System Achieva machine. The following sequences were acquired: (a) dual-echo (DE) turbo spin-echo (repetition time [TR] = 3,125 ms, echo time [TE] = 20/100 ms, echo train length = 6, 44 axial slices, thickness = 3 mm with no gap, matrix size =256 × 247, field of view [FOV] = 240 × 232 mm^2, voxel size = 0.94 × 0.94 × 3 mm, in-plane sensitivity encoding [SENSE] parallel reduction factor = 1.5); (b) three-dimensional (3D) sagittal T1-weighted Turbo Field Echo (TFE) (frequency direction = anterior–posterior; TR = 7.1 ms, TE = 3.3 ms, inversion time [TI] = 1,000 ms, flip angle = 8°, matrix size = 256 × 256 × 180 [inferior–superior, anterior–posterior, left–right], FOV = 256 × 256 mm^2, section thickness = 1 mm; voxel size = 1 × 1 × 1 mm, out-of-plane SENSE parallel reduction factor = 1.5, sagittal orientation); and (c) gradient-echo (GRE) echo planar imaging (EPI) for resting state fMRI (TR = 3,000 ms, TE = 35 ms, flip angle = 90°, matrix size = 128x128, FOV = 240 × 240 mm^2; 200 volumes, 30 contiguous axial slices, slice thickness = 4 mm). During resting state fMRI scanning, participants were instructed to keep as motionless as possible and to keep their eyes closed.

2.3 | MRI analysis

MRI analysis was performed at the Neuroimaging Research Unit, IRCCS Scientific Institute San Raffaele, Milan, Italy.

2.3.1 | Resting state fMRI preprocessing

Resting state fMRI data processing was carried out using the FMRIB software library (FSLv5.0). First, T1-weighted images were skull stripped using the Brain Extraction Tool and segmented in GM, WM, and cerebrospinal fluid (CSF) maps using the FMRIB's Automated Segmentation Tool. Resulting images were registered into the resting state fMRI native space of each subject through a 12 degree of freedom (DOF) linear affine transformation using FMRIB's Linear Image Registration Tool. The first four volumes of the fMRI data were removed to reach complete magnet signal stabilization. Then, individual resting state fMRI images were processed using MELODIC (Multivariate Exploratory Linear Optimized Decomposition into Independent Components; version 3.10; http://www.fmrib.ox.ac.uk/fsl/melodic/; Beckmann, DeLuca, Devlin, & Smith, 2005).The following FSL-standard preprocessing pipeline was applied: (a) motion correction using MCFLIRT; (b) high-pass temporal filtering (lower frequency: 0.01 Hz); (c) spatial smoothing (Gaussian Kernel of FWHM 6 mm); (d) single-session independent component analysis-based automatic removal of motion artifacts (ICA_AROMA; Pruim et al., 2015) in order to identify those independent components (ICs) representing motion-related artifacts. This method calculates a set of spatial and temporal discriminative features and, according to them, exploits a classification procedure to identify ICs representing motion artifacts. Specifically, these features evaluate the spatial overlaps of each component with the edges of brain and CSF, and the frequency content and the temporal correlation with realignment parameters of the IC time-series. In order to check the head motion parameters across the groups, we compared groups based on the four temporal and spatial features of head motion provided by ICA_AROMA (maximum correlation with realignment parameters, edge and CSF fraction and high-frequency content) and we observed no differences (Table S1). Finally, ICs classified as motion-related were re-moved from the fMRI dataset by means of linear regression.

2.3.2 | Seed-based resting state FC (for a brief overview of the method see Figure S1)

Nine regions of interest (ROIs; Figure 1) were created as main nodes of the affective-cognitive network based on previous knowledge (see Introduction): vmPFC, rTPJ, dorsal ACC (dACC), bilateral amygdala and thalamic MDN, and bilateral affective-cognitive part of the cerebellum (AC-cerebellum). All seeds but the amygdala (which was created in the subject native T1-weighted space) were defined in the MNI space and moved to each subject native T1-weighted space trough a specific procedure (see full details below). All ROIs were then visually inspected in the individual brains by neuroimaging expert researchers (EC, FA, AI). Seeds were defined as follows:
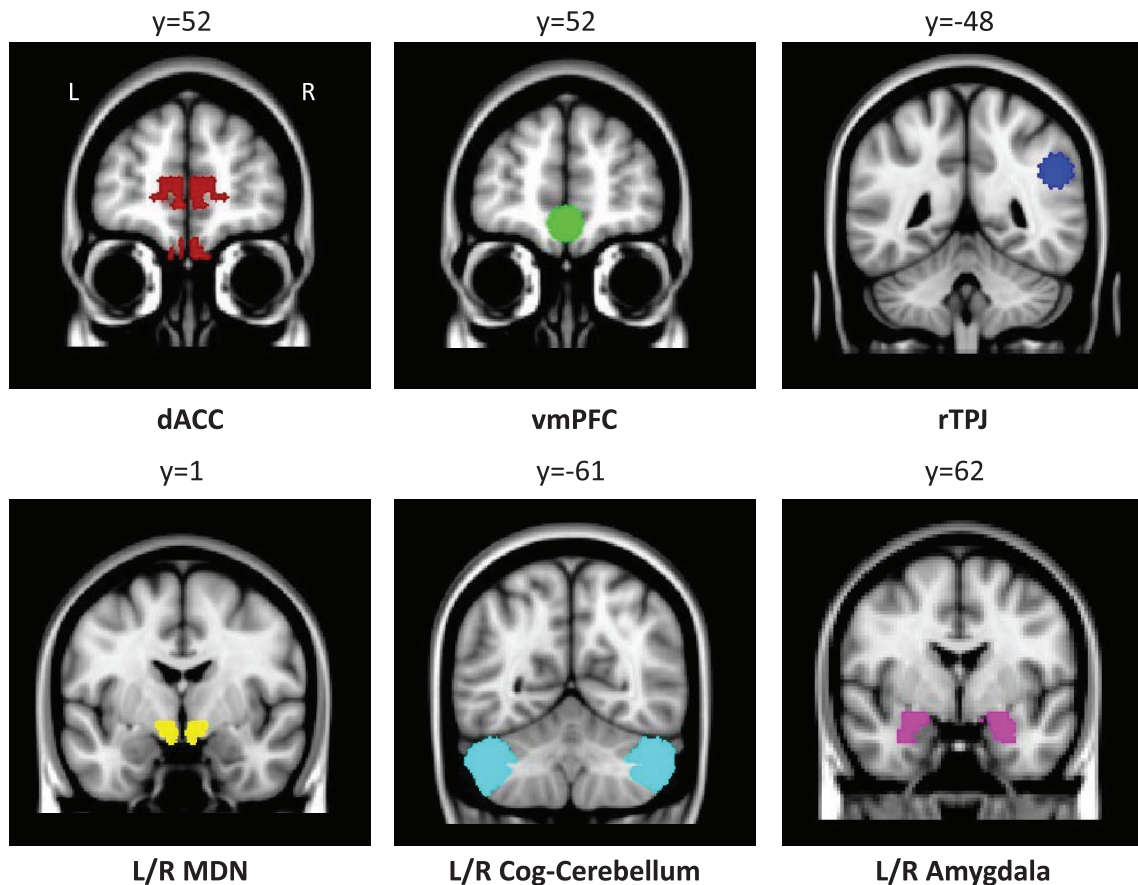
FIGURE 1 Functional connectivity seeds of interest within the affective-cognitive network. Seeds of interest: dorsal anterior cingulate cortex (dACC, red), ventromedial prefrontal cortex (vmPFC, green), right temporoparietal junction (rTPJ, blue), bilateral thalamic medial dorsal nucleus (MDN, yellow), affective-cognitive part of cerebellum (AC-cerebellum, Crus I-II, cyan), and bilateral amygdala (pink). Seeds are overlaid on the Montreal Neurological Institute template in neurological convention (right is right). L, left; R, right

vmPFC

According to a previous fMRI study (Cojan et al., 2009), vmPFC ROI was created as a 10 mm radius sphere centered at the MNI coordinates "x0, y48, z-12" using MarsBaR ROI toolbox for SPM (SPM12).

Right TPJ

rTPJ ROI definition was based on a previous meta-analysis of neuroimaging studies investigating the role of the rTPJ in the sense of self-agency (Decety & Lamm, 2007). rTPJ ROI was created as a 10 mm radius sphere centered at the MNI coordinates "x51, y-46, z31" (the average of MNI coordinates of the 15 studies in the meta-analysis) using MarsBaR ROI toolbox. For studies providing Talairach coordinates, we converted them to MNI space using an appropriate tool from the BioImage suite website (http://sprout022.sprout.yale.edu/mni2tal/mni2tal.html).

dACC and thalamic MDN

Based on anatomical knowledge, these ROIs were defined using the automatic Talairach Daemon (TD) atlas in WFU PickAtlas (Lancaster et al., 2000), toolbox of SPM12. For the dACC, the entire Broadmann area (BA) 32 was considered.

Amygdala

The bilateral amygdala was automatically segmented in the native 3D T1-weighted space using FMRIB's Integrated Registration and Segmentation Tool (FIRST) in FSL (http://www.fmrib.ox.ac.uk/fsl/first) as previously described (Markovic et al., 2017).

AC-cerebellum

The functional distinction of cerebellum into "pure motor" and "affective-cognitive" parts was made according to its projections to different cortical regions (Balsters, Laird, Fox, & Eickhoff, 2014; O'Callaghan et al., 2016). The "affective-cognitive" cerebellum consists of Crus I and II, which project to prefrontal and parietal cortices (Balsters et al., 2014; O'Callaghan et al., 2016). The AC-cerebellum ROI (i.e., the combination of Crus I and II) was obtained from the probabilistic cerebellar atlas (Diedrichsen, Balsters, Flavell, Cussans, & Ramnani, 2009) in the FMRIB software library (FSLv5.0).

Seed-based FC was then performed using a two-step regression analysis as implemented in the FMRIB software library (FSLv5). For a brief overview of the method, see Figure S1. First, time series of WM, CSF, and whole brain volumes in resting state fMRI native space were extracted from the preprocessed and denoised data and their effects were regressed out

using the FMRI Expert Analysis Tool. All seeds of interest were registered to each subject resting state fMRI native space, through the following procedure: a nonlinear registration was calculated from each seed space (MNI) to individual T1-weighted image. Then a 12 DOF linear affine transformation was calculated from individual T1-weighted to individual EPI images. The two registrations were then applied to the starting seeds using the "applywarp" FSL command. ROI mean time-series were calculated. As previously suggested (Inuggi et al., 2014), all ROI time-series were inserted as regressors in the same general linear model and orthogonalized with respect to each of the others according to the Gram Schmidt process implemented in FSL. Considering that these ROIs belong to a same cortico-striatal network, the orthogonalization was imposed to ensure that their time series reflected their unique variance, being confident that this approach does not lead to underestimation of FC because of removal of common variation, or artifactual generation of negative correlations (Inuggi et al., 2014). The output of this step is represented by subject-level maps of all positively and negatively predicted voxels for each regressor. Subject-level maps were registered to the MNI standard template by the applywarp command, after having inverted the two transformations previously calculated.

Resting state network FC: IC analysis

After we removed ICs classified as motion-related, resulting fMRI dataset was high-pass filtered (cutoff frequency of 0.01 Hz) and co-registered to the participant's 3D T1-weighted TFE image using affine boundary-based registration as implemented in FLIRT (Greve & Fischl, 2009; Jenkinson & Smith, 2001) and subsequently transformed to the MNI152 standard space with 4 mm isotropic resolution using nonlinear registration through FNIRT (Andersson, Jenkinson, & Smith, 2007). Preprocessed fMRI data, containing 196 time-points for each subject, were temporally concatenated across subjects to create a single 4D dataset. This fMRI dataset was then decomposed into ICs with a free estimate of the number of components using MELODIC (Multivariate Exploratory Linear Optimized Decomposition into ICs) (Beckmann et al., 2005). In order to identify the subject-specific temporal dynamics and spatial maps associated with each group IC, a dual regression analysis was applied (Filippini et al., 2009). Among group-IC spatial maps, ICs of interest (default mode, visual associative, sensorimotor, cerebellar, executive control, dorsal attention, salience networks) were selected by visual inspection based on previous literature by neuroimaging experts (EC, FA, AI; Smith et al., 2009; Figure S2). Then, dual-regression procedure was performed, which involves: (a) the use of the selected group-IC spatial maps in a linear model fit (spatial regression) against the single subject fMRI data sets, resulting in matrices describing temporal dynamics for each IC and subject and (b) the use of these time-course matrices which are entered into a linear model fit (temporal regression) against the associated fMRI data set to estimate subject-specific spatial maps (Filippini et al., 2009).

2.4 | Statistical analysis

2.4.1 | Demographic and clinical data

Group comparisons were performed using analysis of variance models (SAS Release 9.3, SAS Institute, Cary, NC). Analyses were thresholded at $p < .05$ corrected for multiple comparisons using the false discovery rate.

2.4.2 | Seed-based resting state FC and correlations with clinical findings

Between group differences were tested using the FMRIB's Local Analysis of Mixed Effects (FLAME), which allows multi-level modeling for resting state fMRI group analysis. FC was investigated in each patient group versus the other and versus the group of matched-controls using a general linear model, which includes all groups as independent factors (FixFD, yHC, MobFD, and oHC FC). Between-group comparisons were tested using an interaction analysis: the first interaction model tested the following: [(yHC > FixFD) > (oHC > MobFD)], i.e., −1 1 1−1; the second interaction model tested the following: [(yHC > FixFD) < (oHC > MobFD)], i.e., 1 −1 −1 1. In each FD group, correlations were investigated using FLAME in order to assess the relationship of FC with disease duration, and scores of motor (UDRS, BFMRS, BFMRS-Dys, PMDS) and psychiatric clinical scales (HAMD, HAMA, AS, DES-II, SDQ-20). General linear models were obtained, which included patients' FC maps as dependent variable and aforementioned scores as covariate. Corrections for multiple comparisons were carried out at a cluster level using Gaussian random field theory, $z > 2.3$; cluster significance: $p < .05$, corrected (Worsley et al., 1996).

2.4.3 | Resting state network FC: IC analysis

After the dual regression, spatial maps of all subjects were collected into single 4D files for each original IC. Between-group connectivity differences within RSN of interest were carried out with nonparametric permutation tests (5,000 permutations). The interaction analysis was assessed as described above (see paragraph "Seed-based resting state functional connectivity"). Furthermore, analyses were restricted within the spatial RSN of interest using binary masks obtained by thresholding the corresponding Z map image (Z > 2.3). A family wise error (FWE) correction for multiple comparisons was performed, implementing the threshold-free cluster enhancement using a significance threshold of $p < .05$.

All MRI analyses were adjusted for age and sex.

3 | RESULTS

3.1 | Clinical and demographic features

Each FD group was similar to the corresponding control group in term of age and sex, but they differed in years of education (Table 1). Compared to MobFD, patients with FixFD were similar in sex and years of education, but they were younger, with younger age at disease onset, more pronounced dystonia severity, as well as disability due to dystonia, and less effective botulinum toxin treatment (Table 1).

Additionally, pain was more frequent and CRPS was exclusively present in FixFD group (Table 1). The two groups of patients did not differ in cognitive nor psychiatric features, however psychoactive treatment was more frequent in FixFD cases (Table 1). According to DSM-V criteria, patients with FD had the following psychiatric comorbidities: depressive disorders (17/40), anxiety disorders (2/40), substance-related and addictive disorders (1/40), schizophrenia spectrum and other psychotic disorders (3/40), and personality disorders (2/40).

3.2 | Seed-based resting state FC

3.2.1 | Group comparisons

Between group comparisons in each FC map yielded the following results:

vmPFC
Compared to HC, all FD patients showed reduced connectivity between the vmPFC and left dorsal ACC, and enhanced connectivity between the vmPFC and the left striatum and the Crus I and VI of the cerebellum (Table 2; Figure 2). Compared to oHC, MobFD patients showed reduced connectivity between the vmPFC and right visual associative cortex (Table 2; Figure 3). Compared to yHC, FixFD patients showed reduced connectivity between the vmPFC and the left dorsal ACC, left primary motor cortex, left premotor cortex and supplementary motor area (SMA), and enhanced connectivity between the vmPFC and the left striatum (Table 2; Figure 4). No FC differences were observed between patient groups.

rTPJ
Compared to HC, all FD patients showed reduced connectivity between the rTPJ and left dorsal and rostral PFC (Table 2; Figure 2). Compared to oHC, MobFD patients showed reduced connectivity between the rTPJ and left rostral PFC, and enhanced connectivity between the rTPJ and the right primary somatosensory cortex and caudate (Table 2; Figure 3). Compared to yHC, FixFD patients showed reduced connectivity between the rTPJ and the left premotor cortex and SMA (Table 2; Figure 4). Compared to MobFD, FixFD patients showed reduced connectivity between rTPJ and left frontal eye field (Table 2; Figure 5).

dACC
Compared to HC, all FD patients showed reduced connectivity between the dACC and the right putamen and insula (Table 2; Figure 2). Compared to yHC, FixFD patients showed reduced connectivity between the dACC and the primary motor cortex bilaterally, left primary motor and somatosensory cortices, left supramarginal gyrus, right putamen, right superior temporal, and fusiform gyri (Table 2; Figure 4). Compared to MobFD, FixFD group showed reduced connectivity between the dACC and the bilateral primary and premotor cortices, bilateral SMA and supramarginal gyrus, left fusiform, and

visual associative cortices (Table 2; Figure 5). No FC changes were observed between MobFD and oHC groups.

Left thalamic MDN
Compared to HC, all FD patients showed reduced connectivity between the left MDN and right thalamus (Table 2; Figure 2). Compared to oHC, MobFD group showed reduced connectivity between the left MDN and the bilateral thalamus and the right retrosplenial cortex, and enhanced connectivity between the left MDN and right primary somatosensory cortex, right posterior cingulate cortex and right associative somatosensory cortex, and left visual associative cortex (Table 2; Figure 3). Compared to yHC, FixFD patients showed reduced connectivity between the left MDN and right primary and associative visual cortices, and left superior parietal lobule (Table 2; Figure 4). Compared to MobFD, FixFD patients showed reduced connectivity between the left MDN and the bilateral visual associative cortices, right superior parietal lobule, posterior cingulate cortex and angular gyrus (Table 2; Figure 5).

Right thalamic MDN
Compared to HC, all FD patients showed reduced connectivity between the right MDN and right rostral PFC and insula, and left ventral ACC (Table 2; Figure 2). Compared to oHC, MobFD patients showed enhanced connectivity between the right MDN and the left visual associative cortex (Table 2; Figure 3). Compared to yHC, FixFD patients showed reduced connectivity between the right MDN and the bilateral ventral ACC, right anterior PFC, right premotor cortex and SMA (Table 2; Figure 4). No FC differences were observed between patient groups.

Left AC-cerebellum
Compared to oHC, MobFD patients showed reduced connectivity between left AC-cerebellum and right primary motor cortex, and enhanced connectivity between left AC-cerebellum and left dorsolateral PFC (Table 2; Figure 3). No FC changes were observed between the other groups.

Right AC-cerebellum
Compared to HC, all FD patients showed reduced connectivity between the right AC-cerebellum and the left primary somatosensory cortex, and enhanced connectivity between the right AC-cerebellum and right supramarginal gyrus, left precuneus and angular gyrus (Table 2; Figure 2). Compared to oHC, MobFD group showed enhanced connectivity between the right AC-cerebellum and the precuneus bilaterally, right superior parietal lobule bilaterally, and left supramarginal gyrus (Table 2; Figure 3). Compared to yHC, FixFD patients showed reduced connectivity between the right AC-cerebellum and left primary somatosensory cortex, and enhanced connectivity between the right AC-cerebellum and the right supramarginal gyrus (Table 2; Figure 4). Compared to MobFD, FixFD patients showed reduced connectivity between the right AC-cerebellum and the left primary sensory and supramarginal cortices, left premotor cortex and SMA (Table 2; Figure 5).

TABLE 2 Between group comparisons of seed-based functional connectivity

	Region	N of voxels	Z	x	y	z
vmPFC						
FD < HC	L dorsal ACC	652	4.70	−8	46	16
FD > HC	L caudate	336	3.36	−14	16	8
	L putamen	336	3.35	−20	12	−8
	L cerebellum (crus I/lobule VI)	277	3.92	−12	−78	−22
MobFD<oHC	R visual associative cortex	274	4.25	18	−86	2
FixFD<yHC	L dorsal ACC	458	4.85	−8	46	16
	L premotor and SMA	247	3.25	−56	6	34
	L primary motor cortex	247	3.14	−50	−12	32
FixFD>yHC	L caudate	334	3.50	−16	14	8
	L putamen	334	3.24	−20	12	−8
rTPJ						
FD<HC	L dorsal PFC	579	4.30	−40	10	42
	L rostral PFC	291	3.32	−22	54	12
MobFD<oHC	L rostral PFC	413	4.21	−22	48	18
MobFD>oHC	R primary somatosensory cortex	550	4.35	40	−24	38
	R caudate	397	4.40	12	18	12
FixFD<yHC	L premotor and SMA	564	3.59	−32	−2	52
FixFD<MobFD	L frontal eye field	234	3.93	−20	22	48
dACC						
FD<HC	R putamen	582	4.75	30	−10	−6
	R insula	582	4.25	39	−4	0
FixFD<yHC	R superior temporal gyrus	1,575	4.71	54	−24	4
	R primary motor cortex	1,575	4.20	54	−6	30
	R putamen	1,575	3.98	30	−10	−6
	L primary somatosensory cortex	487	3.49	−58	−14	36
	L primary motor cortex	487	3.27	−48	−10	30
	L supramarginal gyrus	487	3.74	−54	−22	34
	R fusiform gyrus	325	3.65	40	−62	−10
FixFD<MobFD	R primary motor cortex	772	4.21	56	−4	30
	R supramarginal gyrus	772	3.80	56	−26	42
	R primary somatosensory cortex	772	3.72	50	−24	42
	R premotor cortex and SMA	772	3.59	54	−8	42
	L primary somatosensory cortex	314	3.80	−56	−16	36
	L primary motor cortex	314	3.68	−58	−10	22
	L supramarginal gyrus	314	3.56	−54	−22	34
	R premotor cortex and SMA	314	3.55	−52	−4	36
	L fusiform gyrus	282	3.88	−28	−64	−8
	L visual associative cortex	282	3.34	−32	−86	2
Left MDN						
FD < HC	R thalamus, prefrontal connections	225	3.50	12	−18	4
MobFD<oHC	R thalamus, prefrontal connections	482	4.10	6	−22	4
	L thalamus, prefrontal connections	482	3.33	−10	−12	2
	R retrosplenial cortex	482	3.23	16	−38	2

TABLE 2 (Continued)

	Region	N of voxels	Z	x	y	z
MobFD>oHC	R primary somatosensory cortex	324	4.08	40	−28	42
	R posterior cingulate	303	3.58	16	−60	36
	L visual associative cortex	281	4.17	−22	−78	−8
	R associative somatosensory cortex	213	4.16	24	−44	56
FixFD<yHC	L superior parietal lobule	581	4.73	28	−78	36
	R visual associative cortex	245	4.01	6	−82	−2
FixFD<MobFD	R precuneus/superior parietal	767	4.71	10	−66	32
	R dorsal PCC	767	4.34	14	−62	36
	R angular gyrus	767	3.81	36	−68	42
	L visual associative cortex	431	4.27	−16	−74	34
	L visual associative cortex	417	3.78	−20	−78	−10
	R visual associative cortex	237	3.74	12	−80	−10
	R primary visual cortex	237	3.26	14	−92	4
Right MDN						
FD<HC	R rostral PFC	470	3.98	0	56	8
	L ventral ACC	271	3.15	−4	−8	30
	R insula	266	3.59	36	22	0
MobFD>oHC	L visual associative cortex	430	4.21	−24	−56	−6
FixFD<yHC	L ventral ACC	389	3.19	−8	−4	38
	R anterior prefrontal cortex	258	4.43	0	62	6
	R ventral ACC	235	3.10	8	−4	32
	R premotor and SMA	235	2.96	42	−2	32
Left AC-cerebellum						
MobFD<oHC	R primary somatosensory cortex	387	4.10	36	−16	39
MobFD>oHC	L dorsolateral PFC	256	4.62	−46	26	34
Right AC-Cerebellum						
FD<HC	L primary somatosensory gyrus	694	3.91	−34	16	30
FD>HC	R supramarginal gyrus	1,382	4.32	44	−52	52
	L precuneus	1,382	4.28	−40	−44	54
	L angular gyrus	1,382	3.52	−38	−54	56
MobFD>oHC	R precuneus	376	3.97	18	−66	46
	R superior parietal lobule	279	3.77	36	−50	54
	L precuneus	259	4.02	−22	−64	52
	L supramarginal gyrus	232	4.29	−48	−34	44
FixFD<yHC	L primary somatosensory cortex	431	3.63	−34	−26	46
FixFD>yHC	R supramarginal gyrus	344	4.17	44	−52	52
FixFD<MobFD	L primary somatosensory cortex	276	5.29	−34	−26	46
	L supramarginal gyrus	276	3.99	−46	−34	44
	L premotor and SMA	424	3.33	−30	2	48
Left amygdala						
FD>HC	L thalamus	287	4.11	−10	−8	4
	R thalamus	287	3.61	12	−6	4
	L precuneus	233	3.47	−2	−68	48
FixFD>yHC	L precuneus	461	3.36	−4	−68	40
	R dorsal PCC	461	3.31	4	−58	34

(Continues)

TABLE 2 (Continued)

	Region	N of voxels	Z	x	y	z
Right amygdala						
MobFD>oHC	R thalamus, prefrontal connections	324	3.79	17	−12	8
	R putamen	324	3.10	30	−13	8
	R anterior PFC	215	3.77	30	50	16
	R angular gyrus	220	3.50	52	−48	14

Note: Coordinates (*x, y, z*) are in Montreal Neurological Institute (MNI) space. Results are shown at *p* < .05, family wise error (FWE) corrected for multiple comparisons implementing the threshold-free cluster enhancement, adjusting for age and sex.

Abbreviations: AC-Cerebellum, affective-cognitive part of cerebellum (Crus I and II); ACC, anterior cingulate cortex; BA, Brodmann area; dACC, dorsal anterior cingulate cortex; FixD, fixed dystonia; yHC, young healthy controls; L, left; MDN, thalamic medial dorsal nucleus; MobD, mobile dystonia; oHC, old healthy controls; PFC, prefrontal cortex; R, right; rTPJ, right temporo-parietal junction; SMA, supplementary motor area; vmPFC, ventromedial prefrontal cortex.
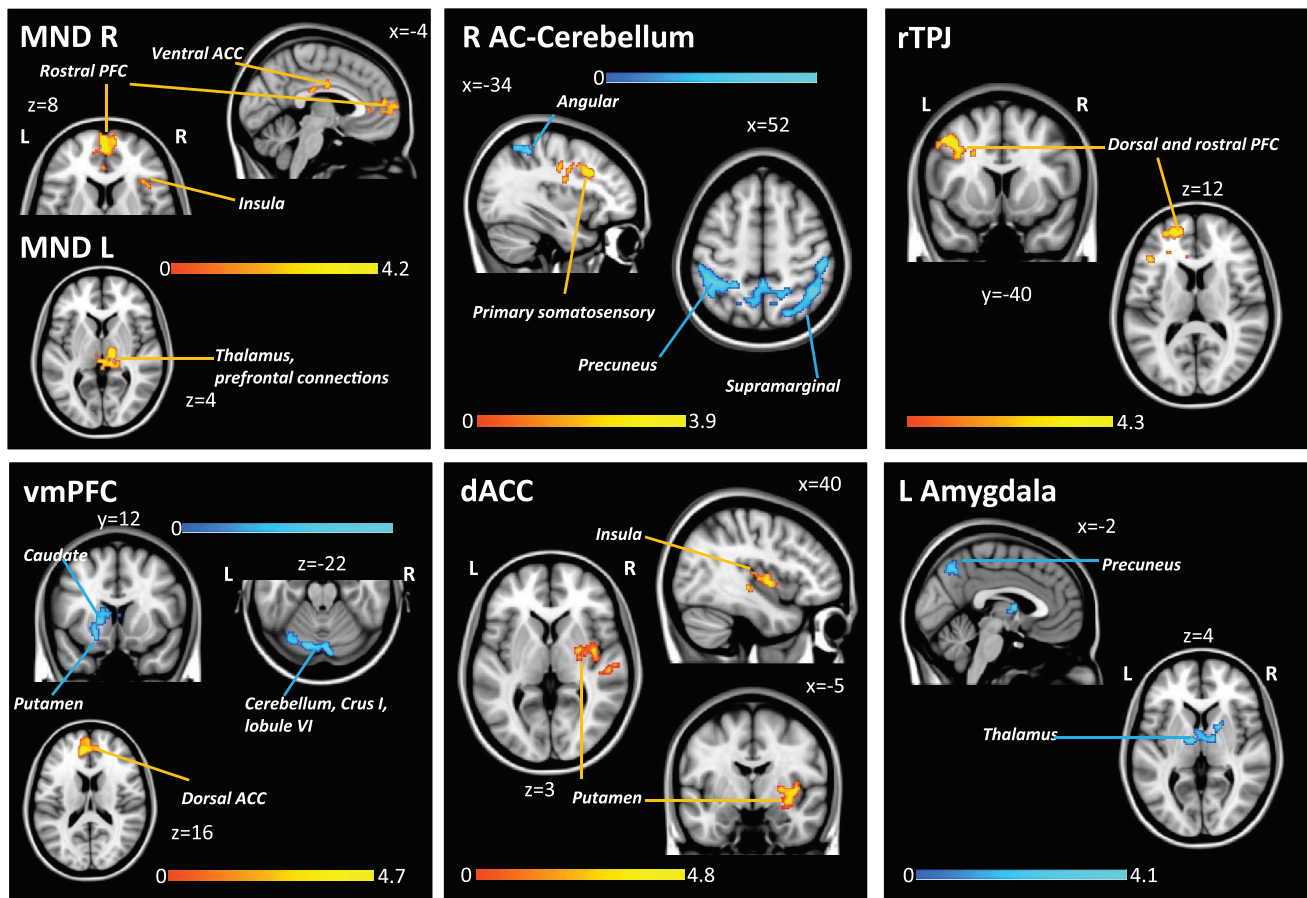
FIGURE 2 Regions where all FD patients showed enhanced (cold colors) or reduced (warm colors) functional connectivity with the affective-cognitive network brain regions compared to healthy controls. Results are overlaid on the Montreal Neurological Institute template in neurological convention (right is right), displayed at *p* < .05 family wise error corrected for multiple comparisons, implementing the threshold-free cluster enhancement. Colored bar represents *Z*-values. AC-cerebellum, affective-cognitive part of cerebellum; ACC, anterior cingulate cortex; FD, functional dystonia; HC, healthy controls; L, left; MDN, medial dorsal nucleus of thalamus; PCC, posterior cingulate cortex; PFC, prefrontal cortex; R, right; rTPJ, temporo-parietal junction; vmPFC, ventromedial prefrontal cortex
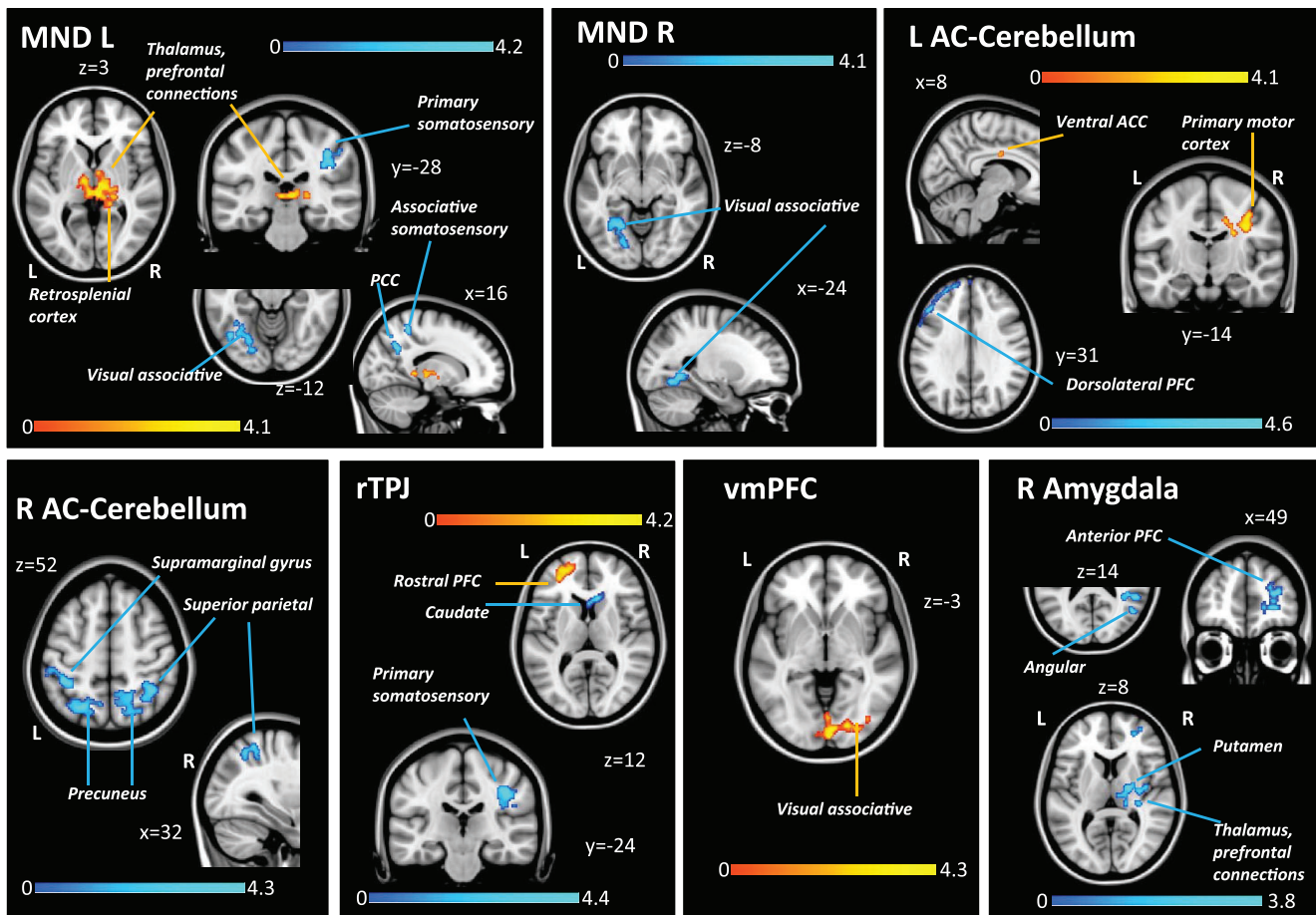
FIGURE 3 Regions where MobFD patients showed enhanced (cold colors) or reduced (warm colors) functional connectivity with the affective-cognitive network brain regions compared to healthy controls. Results are overlaid on the Montreal Neurological Institute template in neurological convention (right is right), displayed at *p* < .05 family wise error corrected for multiple comparisons, implementing the threshold-free cluster enhancement. Colored bar represents *Z*-values. AC-cerebellum, affective-cognitive part of cerebellum; ACC, anterior cingulate cortex; HC, healthy controls; L, left; MDN, medial dorsal nucleus of thalamus; MobFD, mobile functional dystonia; PCC, posterior cingulate cortex; PFC, prefrontal cortex; R, Right; rTPJ, temporo-parietal junction; vmPFC, ventromedial prefrontal cortex

Left amygdala

Compared to HC, all FD patients showed enhanced connectivity between the left amygdala and the thalamus bilaterally, and the left precuneus (Table 2; Figure 2). Compared to yHC, FixFD patients showed enhanced connectivity between the left amygdala and the right PCC and left precuneus (Table 2; Figure 4). No FC changes were observed between the other groups.

Right amygdala

Compared to oHC, MobFD patients enhanced connectivity between the right amygdala and the right prefrontal connections of thalamus, right putamen, anterior PFC and angular gyrus (Table 2; Figure 3). No FC changes were observed between the other groups.

3.2.2 | Clinical-MRI correlations

MobFD patients showed a significant positive correlation between disease duration and FC of the vmPFC with the left anterior thalamic radiations. No other significant correlations were found.

3.3 | Resting state network FC: IC analysis

Compared to controls and MobFD patients, FixFD patients showed reduced connectivity of the left Crus regions I and lobule VI of the cerebellum and of the vermis bilaterally within the cerebellar network (Table 3; Figure 6). No FC changes were observed within the other resting state networks.
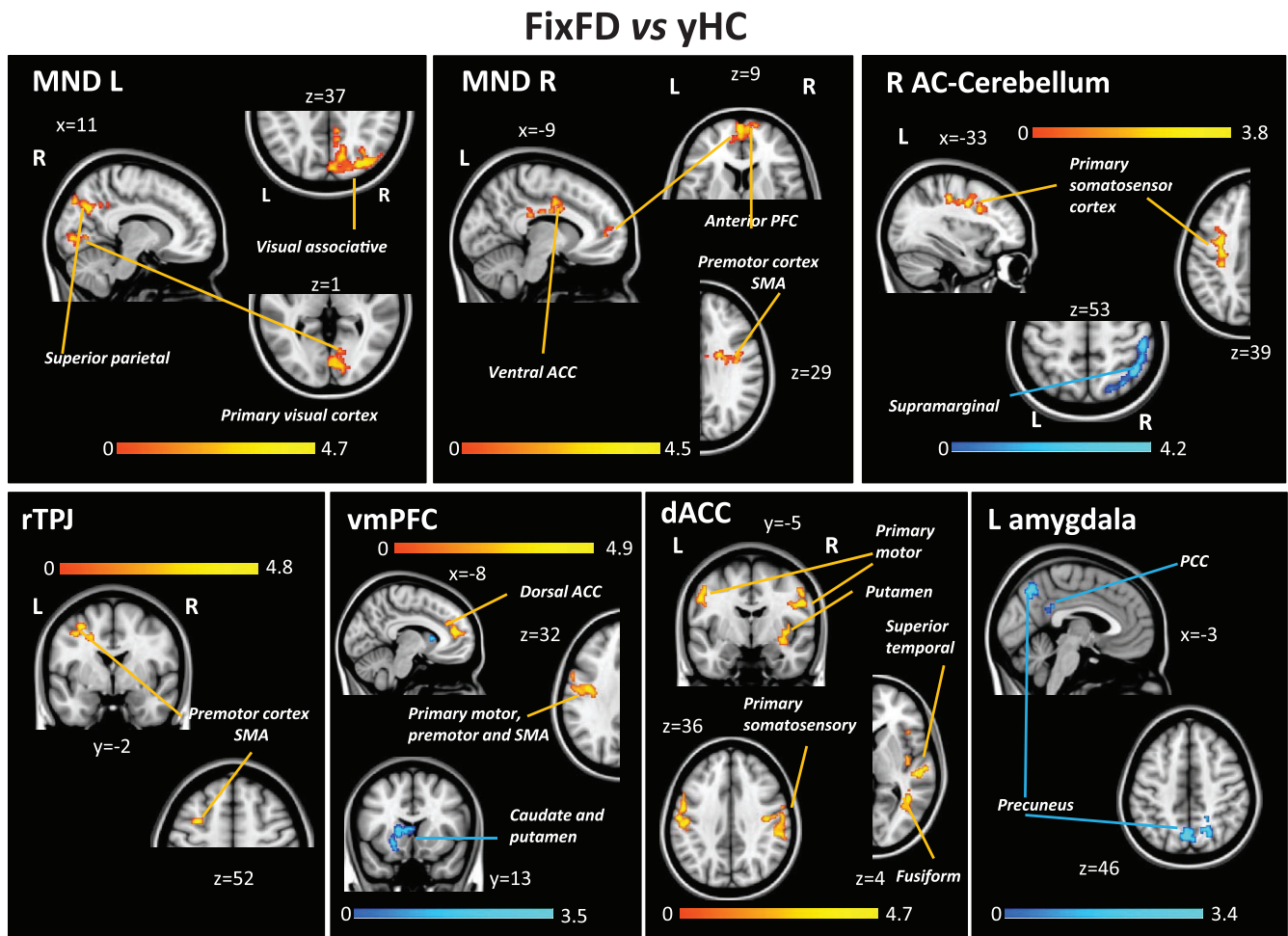
FIGURE 4 Regions where FixFD patients showed enhanced (cold colors) or reduced (warm colors) functional connectivity with the affective-cognitive network brain regions compared to healthy controls. Results are overlaid on the Montreal Neurological Institute template in neurological convention (right is right), displayed at $p < .05$ family wise error corrected for multiple comparisons, implementing the threshold-free cluster enhancement. Colored bar represents Z-values. AC-cerebellum, affective-cognitive part of cerebellum; ACC, anterior cingulate cortex; dACC, dorsal anterior cingulate cortex; FixFD, fixed functional dystonia; L, left; MDN, medial dorsal nucleus of thalamus; PFC, prefrontal cortex; R, right; rTPJ, temporo-parietal junction; SMA, supplementary motor area; vmPFC, ventromedial prefrontal cortex

4 | DISCUSSION

In this study, three major points emerged: (a) compared with HC, all FD patients shared a common pattern of reduced connectivity between the majority of affective-cognitive seeds of interest and the fronto-subcortical and limbic circuits, enhanced connectivity of the right AC-cerebellum with the associative cortices, and enhanced connectivity of the bilateral amygdala with the subcortical and posterior cortical brain regions; (b) both groups of patients showed an aberrant connectivity between the MDN and the sensorimotor and associative brain regions when compared with HC but with an opposite pattern (enhanced connectivity in MobFD and reduced in FixFD); (c) in general, compared with yHC and MobFD patients, FixFD group had an extensive pattern of reduced FC within the cerebellar network and between the majority of affective-cognitive seeds of interest and the

sensorimotor and high-order function ("cognitive") areas with a unique involvement of dACC connectivity.

4.1 | AC-cerebellum

The anatomical and functional interconnections of cerebellum with the basal ganglia and cortex, and thus, its influence on motor planning and execution, higher-order cognitive and emotional functions, and behavior (O'Callaghan et al., 2016) are clearly implicated in the pathophysiology of dystonia (Shakkottai et al., 2017). Affective and cognitive sub-regions of the cerebellum are associated with the large-scale cortical networks involved in cognitive and limbic functions, including the executive, salience and default mode networks (O'Callaghan et al., 2016). When compared with controls, in all FD patients, the right
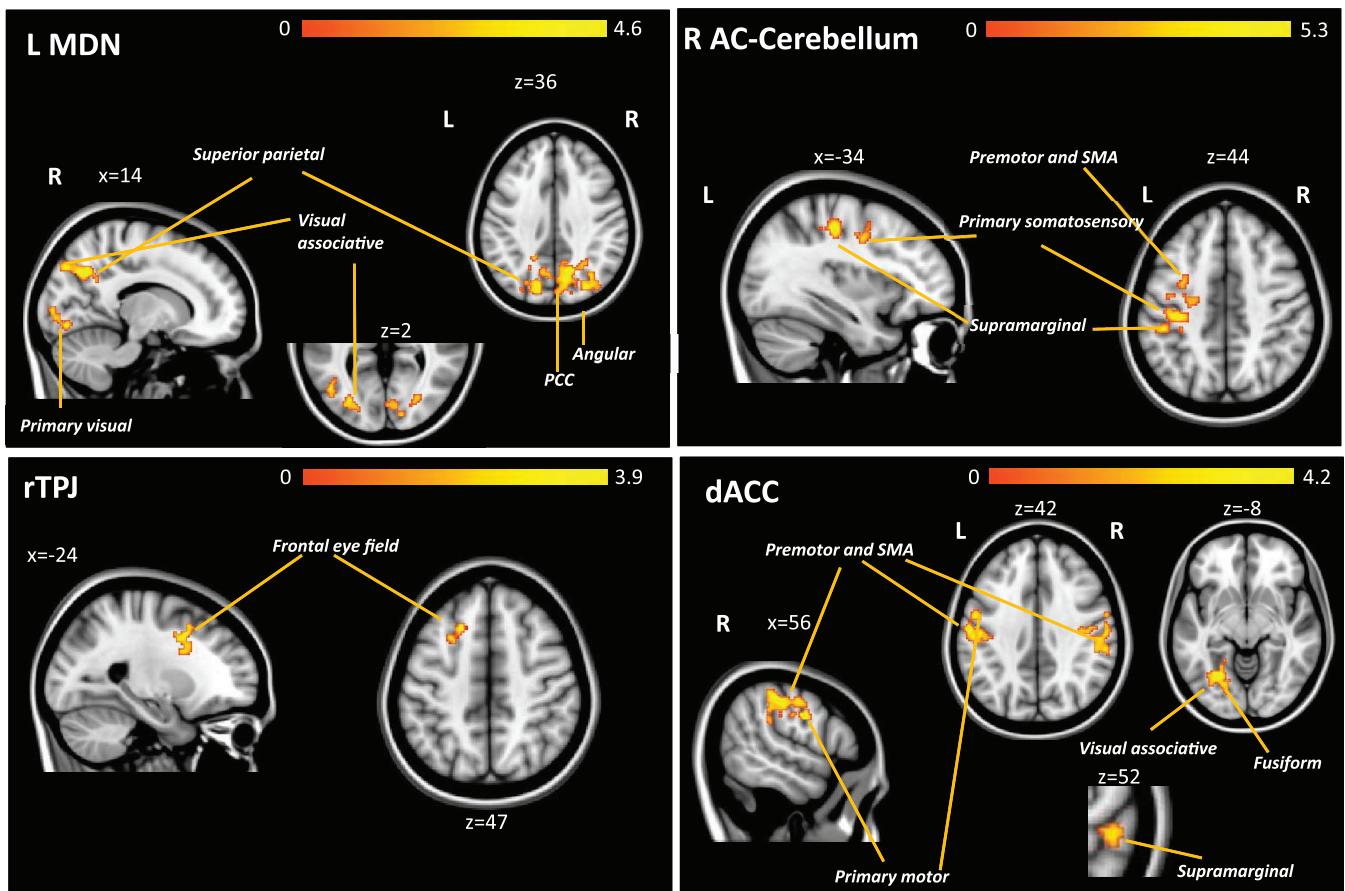
FIGURE 5 Regions where FixFD patients showed reduced functional connectivity with the affective-cognitive network brain regions compared to MobFD patients. Results are overlaid on the Montreal Neurological Institute template in neurological convention (right is right), displayed at *p* < .05 family wise error corrected for multiple comparisons, implementing the threshold-free cluster enhancement. Colored bar represents <u>Z</u>-values. ACC, anterior cingulate cortex; cognitive part of cerebellum, AC-cerebellum; dACC, dorsal anterior cingulate cortex; FixFD, fixed functional dystonia; L, Left; MobFD, mobile functional dystonia; MDN, medial dorsal nucleus of thalamus; PCC, posterior cingulate cortex; rTPJ, temporo-parietal junction; SMA, supplementary motor area

TABLE 3 Between-group connectivity differences within the resting state cerebellar network

	Region	N of voxels	Z	x	y	z
Cerebellar network						
FixD<HC	L crus I/lobule VI	70	3.10	−26	−66	−32
FixD<MobD	L vermis X	61	3.17	−1	−45	−32
	R vermis IX	3	3.46	14	−46	−48

Note: Coordinates (*x, y, z*) are in Montreal Neurological Institute (MNI) space. Results are shown at *p* < .05, family wise error (FWE) corrected for multiple comparisons implementing the threshold-free cluster enhancement, adjusting for age and sex.
Abbreviations: FixD, fixed dystonia; HC, healthy controls; L, left; MobD, mobile dystonia; R, right.

AC-cerebellum showed reduced connectivity (which was also more pronounced in FixFD than MobFD) with left primary sensory cortex, premotor cortex and SMA, and enhanced connectivity (particularly evident in MobFD) with bilateral superior parietal lobule and supramarginal gyrus, reflecting aberrant modulation of primary and associative sensory regions, with possible further disruption of sensorimotor integration. Although we did not observe a relationship between these changes and somatization disturbances in these

patients, parietal lobe dysfunctions are often linked with marked somatoform dissociation as severe that ended-up with limb amputation and were related to apotemnophilia or xenomelia (Edwards et al., 2011; Giummarra, Bradshaw, Nicholls, Hilti, & Brugger, 2011). In the network analysis, we observed that the group of FixFD patients, when compared to the other two groups, showed reduced connectivity within the cerebellar network in both motor and affective control subregions (Crus I/Lobule VI and vermis). An aberrant resting state FC
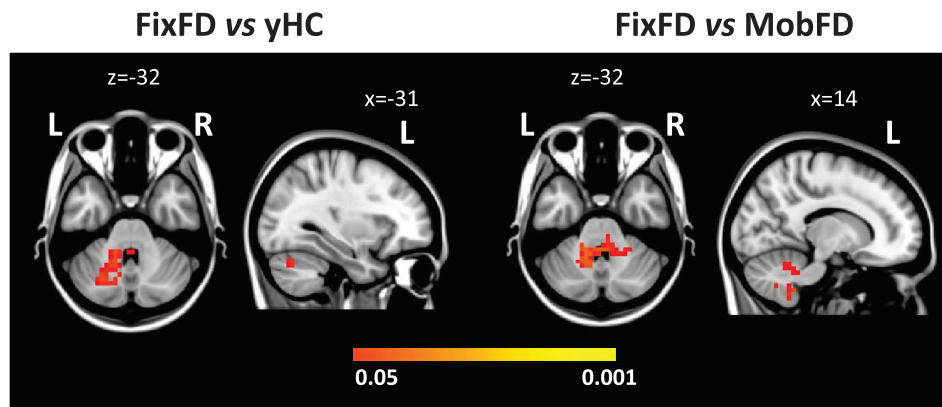
FIGURE 6 Reduced resting state functional connectivity in the investigated networks in FixFD patients compared to healthy controls and to MobFD patients. Results are overlaid on the 3D Montreal Neurological Institute template in neurological convention (right is right) and displayed at $p < .05$ family wise error (FWE) corrected for multiple comparisons implementing the threshold-free cluster enhancement, and adjusted for subject's age and sex. Colored bar represents p-values. HC, healthy controls; FixFD, fixed functional dystonia; L, left; MobFD, mobile functional dystonia; R, right

in the Crus I region has been previously described in the early phases of the somatization process (Wang et al., 2016). Furthermore, the present findings are in line with our previous work (Tomic et al., 2018) where we observed a widespread pattern of structural disconnection that was unique in FixFD patients and involved the entire cerebellar WM. Thus, particularly in these patients, the cerebellar output disruption might be important for determining the occurrence of motor symptoms.

4.2 | dACC

In our study, FC alterations of the dACC were observed in all patients when compared with controls. However, in the subgroup comparisons, they were exclusively observed in FixFD patients. We should stress that when compared FixFD with yHC and MobFD cases, relative to other ROIs, the dACC had widespread functional "disconnection" affecting the primary sensorimotor and higher order motor regions (such as SMA), putamen, insular and visual–auditory associative cortices. Different cingulate activity changes have been described in previous studies of functional neurological disorders (Voon et al., 2010; Wang et al., 2016). More recent neuroimaging studies suggested that ACC subgenual and perigenual subregions are implicated in emotion regulation and fear extinction, while dACC is engaged in emotional appraisal and cognitive control (Etkin, Egner, & Kalisch, 2011). Thus, the dACC, with significant projections to the motor cortex, can act as an interface between sensorimotor and affective-cognitive processing (Friedman et al., 2017). The interaction between dACC with SMA during motor coordination and with primary motor cortex during working memory activities is well known and bidirectional (Diwadkar, Asemi, Burgess, Chowdury, & Bressler, 2017). Specifically, the dACC-SMA connectivity has been observed to increase during motor coordination task and to decrease during rest in healthy young subjects (Diwadkar et al., 2017). During resting state,

our FixFD patients had altered FC between the dACC and the primary motor cortex, premotor region and SMA, which might reflect the loss of control of the dACC over these brain regions with subsequent errors in selection of motor pattern and motor execution, leading to FixFD.

We further observed decreased FC between the dACC and the right insula in FixFD patients when compared with HC. Cingulo-insular volumes were decreased in patients with predominant pain syndrome compared with controls (Valet et al., 2009). Considering that pain in dystonic regions and CPRS are some of the core clinical characteristic FixFD, insular activity changes could promote aberrant pain processing.

4.3 | rTPJ

The rTPJ is implicated in different high-level cognitive processes, such as motor intentional awareness and self-agency (Voon, Gallea, et al., 2010), alien limb syndrome (Graff-Radford et al., 2013), and impairments in body-self integration (i.e., out of body experiences) (De Ridder, Van Laere, Dupont, Menovsky, & Van de Heyning, 2007). Clinically, most of our FixFD patients defined affected extremity as useless, immobile, painful, and not being part of their own body, sometimes resembling to alien limb syndrome. Functional disconnection between the rTPJ and prefrontal (dorsolateral and anterior) and premotor cortex and SMA that we observed particularly in FixFD patients might be the correlate of the loss of sense of agency (i.e., involuntariness/unawareness) and the altered top-down regulation of the highest motor and cognitive control leading to impaired motor intention and execution. Furthermore, enhanced connectivity between rTPJ and right caudate and primary somatosensory cortex in MobFD compared to old HC might modulate fronto-subcortical loops involved in motor intention or attention (Tekin & Cummings, 2002).

4.4 | vmPFC

Prefrontal abnormalities in FD match with equivalent abnormalities in organic dystonia arguing against the hypothesis that they reflect a marker of FD per se (Schrag et al., 2013). However, the critical role of the vmPFC in functional neurological disorders was shown in previous studies, suggesting that abnormal, personally relevant affective information encoded in this region might alter sensorimotor circuit activity (Aybek & Vuilleumier, 2016). Thus, the vmPFC related modulation of motor behavior might be driven by affect, imagery and/or memory related representations. In addition, most task-based fMRI studies in negative motor conversion disorders (i.e., functional paralysis and sensory loss) showed higher activity of the vmPFC in contrast to lower activity of primary sensorimotor regions, suggesting that emotional or motivational processes produced active inhibition of primary sensorimotor cortical areas (Aybek & Vuilleumier, 2016). Furthermore, one study in FMD patients observed a disconnection between prefrontal regions and regions involved in motor preparation (including SMA) during internally versus externally generated action fMRI task providing evidence of impaired top-down regulation of internal action initiation (Voon, Brezing, Gallea, & Hallett, 2011). In line with these findings, in a resting state condition, we found that in particular the FixFD group showed a decreased FC between the vmPFC and the premotor, SMA and superior frontal gyrus. Furthermore, in MobFD patients the connectivity between vmPFC and the associative cortices, rather than with the motor preparation brain regions, was reduced, while the connectivity of the anterior thalamus enhanced with longer disease duration suggesting that in MobFD patients the altered frontal, thalamic and parietal associative circuits modify emotional control over complex somatosensory network (Aybek & Vuilleumier, 2016).

4.5 | Thalamic MDN

The role of the thalamus in pathophysiology of dystonia is well known. However, most of the studies in dystonia referred to sensorimotor part of the thalamus (Neychev, Gross, Lehericy, Hess, & Jinnah, 2011). Apart from its significance in sensorimotor characteristics of dystonia, the midline thalamus, including the MDN, is considered to play a role in cognitive and emotional regulation (Mitchell, 2015). Of note, the MDN, a big associative nucleus, as a part of the basolateral limbic system, has strong interconnections with the medial PFC as well as with the amygdala. As such, it is involved in multiple cognitive processes, but also self-consciousness and behavioral flexibility serving as a bridge in the limbic circuits of learning and memory processes (Lee et al., 2011).

Our FixFD group showed reduced connectivity between the left MDN and the right parietal associative cortex, PCC and primary and associative visual cortex, while the right MDN had lower connectivity with the right ventral ACC, premotor and SMA, and anterior PFC bilaterally. Considering that the MDN serves to enhance prefrontal top-down modulation of selective attention and inhibition of irrelevant stimuli, reduced connectivity between this relay node and the regions involved in sensorimotor integration, motor selection and visuospatial functions suggests possible attention deficit, postulated as main neurobiological paradigm of FMD, with switch of attention towards the body/symptom (Edwards et al., 2013). On the other hand, MobFD patients had an opposite connectivity pattern, that is, enhanced connectivity between bilateral MDN and the PCC, primary and associative sensory cortex, visual associative cortex, supramarginal and fusiform gyri, implicating different selective attention circuit model, with possible significant limbic modulation of higher sensory and cognitive regions. Alternatively, a "functional deafferentation" model has been proposed as a result of active inhibition of somatosensory processing by limbic areas associated with emotion and attention (Espay et al., 2018) that might be relevant for our MobFD patients. Further, decreased FC was found in the thalamus of MobFD patients, mainly in those parts with prefrontal connections. Interestingly, MobFD patients act as other functional neurological disorders exhibiting abnormalities predominantly at subcortical level (Voon, Gallea, et al., 2010; Vuilleumier et al., 2001). Some authors have hypothesized that in FD emotional stressors act via limbic inputs from the orbitofrontal cortex and amygdala to modulate basal ganglia–thalamocortical circuits, leading to a selective deficit of willed action (i.e., the faculty of consciously making a choice or selecting an action; Vuilleumier et al., 2001). Although the communication between the MDN and PFC seems to be critical for flexible choice behavior (Vertes et al., 2015), it remains to be clarified whether disrupted behavioral flexibility might be related to pathophysiology of fixed and permanent or mobile and variable motor pattern.

4.6 | Amygdala

The amygdala is a crucial structure in the modulation of motivated attention and preparation for action. Previous studies showed that arousing stimuli increased amygdala connectivity during motor initiation in patients with motor conversion disorders (Voon et al., 2010; Voon et al., 2011). Our data confirmed that even during rest, the amygdala is abnormally hyperactive in its thalamic and precuneal connectivity. Since the basolateral amygdala receives input from the thalamus and cerebral cortex, one might speculate that there is an overexpression of salient previously learned and mapped motor representations (subtended mainly by the precuneus) with the lack of a prefrontal top-down control that we observed in all patients.

Some limitations of our study should be noted. First, FixFD sample was almost three times smaller than MobFD group, which, together with different age, challenged the direct comparison between patient groups and requires caution in discussion. Second, the association of brain findings with their clinical importance was limited to few significant correlations. Larger samples are needed to replicate these findings. Third, a thorough clinical assessment including a comprehensive evaluation of neuropsychological, psychiatric and pain-related features is necessary in interpretation of complex changes affecting cognitive and emotional networks. Fourth, although

we provide a good coverage of the cortical, subcortical and cerebellar components of the affective-cognitive network, we may have not included all possible brain regions involved in the disease. However, the lack of significant findings in other networks assessed using ICA suggests a certain specificity of our results. Fifth, we used a 1.5 T MRI scanner, which is characterized by a lower BOLD signal to noise ratio compared with higher field strength scanners. Finally, an "organic" dystonia group would have been a useful control group for understanding the specific features associated with each type of FD. Future large studies, controlling for the clinical heterogeneous presentations of the different types of dystonia and multiple testing issues, are warranted to complete the picture.

Despite these shortcomings, we showed that aberrant FC among the crucial nodes of the affective-cognitive circuits implicated in motor control presented with different patterns in FixFD and MobFD patients. The FixFD group, neurologically more severe and complex form of FD, therapeutically resistant, with quite poor prognosis, was characterized by a widespread disconnection between the key nodes of the network and different higher order cognitive, emotional, sensory and motor controlling regions. On the other hand, in MobFD patients FC alterations were predominantly defined by a thalamic MDN disconnectivity. In a previous work, we have defined the brain structural alterations of these two clinical presentations of FD. Resembling other FMD disorders (Perez et al., 2015), we observed that MobFD had morphological changes in GM cortical and subcortical structures (Tomic et al., 2018). On the other hand, we found that FixFD had a massive and distributed WM damage (with not GM alterations; Tomic et al., 2018), which resembles a disconnection syndrome comparable to other major psychiatric or neurodegenerative diseases. In line with these findings, we observed a greater reduction of brain FC in FixFD patients compared with MobFD that well reflects the disconnection hypothesis in the FixFD motor pattern. Multiparametric MRI studies specifically designed to assess the relationships between structural and functional brain changes will improve further our knowledge of the two FD presentations.

All these findings suggest an interaction between brain connectivity architecture and clinical expression of FD. The presence of FC changes in this condition might provide evidence of abnormal brain function and hence an organic disorder, arguing against the existence of a "psychogenic" etiology for FD.

CONFLICT OF INTERESTS

DATA AVAILABILITY STATEMENT

The dataset used and analyzed during the current study will be made available by the corresponding author upon request to qualified researchers (i.e., affiliated to a university or research institution/hospital).

ORCID

Massimo Filippi https://orcid.org/0000-0002-5485-0479

REFERENCES

Andersson JL, Jenkinson M, Smith S. 2007. *Non-linear registration, aka spatial normalisation*. FMRIB technical report TR07JA2. Oxford, United Kingdom.

Aybek, S., & Vuilleumier, P. (2016). Imaging studies of functional neurologic disorders. *Handbook of Clinical Neurology*, *139*, 73–84.

Balsters, J. H., Laird, A. R., Fox, P. T., & Eickhoff, S. B. (2014). Bridging the gap between functional and anatomical features of cortico-cerebellar circuits using meta-analytic connectivity modeling. *Human Brain Mapping*, *35*, 3152–3169.

Beckmann, C. F., DeLuca, M., Devlin, J. T., & Smith, S. M. (2005). Investigations into resting-state connectivity using independent component analysis. *Philosophical Transactions of the Royal Society of London. Series B, Biological Sciences*, *360*, 1001–1013.

Boeckle, M., Liegl, G., Jank, R., & Pieh, C. (2016). Neural correlates of conversion disorder: Overview and meta-analysis of neuroimaging studies on motor conversion disorder. *BMC Psychiatry*, *16*, 195.

Botvinick, M., Nystrom, L. E., Fissell, K., Carter, C. S., & Cohen, J. D. (1999). Conflict monitoring versus selection-for-action in anterior cingulate cortex. *Nature*, *402*, 179–181.

Burke, R. E., Fahn, S., Marsden, C. D., Bressman, S. B., Moskowitz, C., & Friedman, J. (1985). Validity and reliability of a rating scale for the primary torsion dystonias. *Neurology*, *35*, 73–77.

Calne, D. B., & Lang, A. E. (1988). Secondary dystonia. *Advances in Neurology*, *50*, 9–33.

Carlson, E. B., Putnam, F. W., Ross, C. A., Torem, M., Coons, P., Dill, D. L., ... Braun, B. G. (1993). Validity of the dissociative experiences scale in screening for multiple personality disorder: A multicenter study. *The American Journal of Psychiatry*, *150*, 1030–1036.

Cojan, Y., Waber, L., Carruzzo, A., & Vuilleumier, P. (2009). Motor inhibition in hysterical conversion paralysis. *NeuroImage*, *47*, 1026–1037.

Comella, C. L., Leurgans, S., Wuu, J., Stebbins, G. T., Chmura, T., & Dystonia Study G. (2003). Rating scales for dystonia: A multicenter assessment. *Movement Disorders*, *18*, 303–312.

de Lange, F. P., Toni, I., & Roelofs, K. (2010). Altered connectivity between prefrontal and sensorimotor cortex in conversion paralysis. *Neuropsychologia*, 48, 1782–1788.

De Ridder, D., Van Laere, K., Dupont, P., Menovsky, T., & Van de Heyning, P. (2007). Visualizing out-of-body experience in the brain. *The New England Journal of Medicine*, 357, 1829–1833.

Decety, J., & Lamm, C. (2007). The role of the right temporoparietal junction in social interaction: How low-level computational processes contribute to meta-cognition. *The Neuroscientist*, 13, 580–593.

Diedrichsen, J., Balsters, J. H., Flavell, J., Cussans, E., & Ramnani, N. (2009). A probabilistic MR atlas of the human cerebellum. *NeuroImage*, 46, 39–46.

Diwadkar, V. A., Asemi, A., Burgess, A., Chowdury, A., & Bressler, S. L. (2017). Potentiation of motor sub-networks for motor control but not working memory: Interaction of dACC and SMA revealed by resting-state directed functional connectivity. *PLoS One*, 12, e0172531.

Edwards, M. J., Alonso-Canovas, A., Schrag, A., Bloem, B. R., Thompson, P. D., & Bhatia, K. (2011). Limb amputations in fixed dystonia: A form of body integrity identity disorder? *Movement Disorders*, 26, 1410–1414.

Edwards, M. J., Fotopoulou, A., & Parees, I. (2013). Neurobiology of functional (psychogenic) movement disorders. *Current Opinion in Neurology*, 26, 442–447.

Espay, A. J., & Lang, A. E. (2015). Phenotype-specific diagnosis of functional (psychogenic) movement disorders. *Current Neurology and Neuroscience Reports*, 15, 32.

Espay, A. J., Maloney, T., Vannest, J., Norris, M. M., Eliassen, J. C., Neefus, E., … Szaflarski, J. P. (2018). Dysfunction in emotion processing underlies functional (psychogenic) dystonia. *Movement Disorders*, 33, 136–145.

Etkin, A., Egner, T., & Kalisch, R. (2011). Emotional processing in anterior cingulate and medial prefrontal cortex. *Trends in Cognitive Sciences*, 15, 85–93.

Filippini, N., MacIntosh, B. J., Hough, M. G., Goodwin, G. M., Frisoni, G. B., Smith, S. M., … Mackay, C. E. (2009). Distinct patterns of brain activity in young carriers of the APOE-epsilon4 allele. *Proceedings of the National Academy of Sciences of the United States of America*, 106, 7209–7214.

Folstein, M. F., Folstein, S. E., & McHugh, P. R. (1975). "Mini-mental state". A practical method for grading the cognitive state of patients for the clinician. *Journal of Psychiatric Research*, 12, 189–198.

Friedman, A. L., Burgess, A., Ramaseshan, K., Easter, P., Khatib, D., Chowdury, A., … Diwadkar, V. A. (2017). Brain network dysfunction in youth with obsessive-compulsive disorder induced by simple uni-manual behavior: The role of the dorsal anterior cingulate cortex. *Psychiatry Research: Neuroimaging*, 260, 6–15.

Giummarra, M. J., Bradshaw, J. L., Nicholls, M. E., Hilti, L. M., & Brugger, P. (2011). Body integrity identity disorder: Deranged body processing, right fronto-parietal dysfunction, and phenomenological experience of body incongruity. *Neuropsychology Review*, 21, 320–333.

Graff-Radford, J., Rubin, M. N., Jones, D. T., Aksamit, A. J., Ahlskog, J. E., Knopman, D. S., … Josephs, K. A. (2013). The alien limb phenomenon. *Journal of Neurology*, 260, 1880–1888.

Greve, D. N., & Fischl, B. (2009). Accurate and robust brain image alignment using boundary-based registration. *NeuroImage*, 48, 63–72.

Gupta, A., & Lang, A. E. (2009). Psychogenic movement disorders. *Current Opinion in Neurology*, 22, 430–436.

Hamilton, M. (1959). The assessment of anxiety states by rating. *The British Journal of Medical Psychology*, 32, 50–55.

Hamilton, M. (1960). A rating scale for depression. *Journal of Neurology, Neurosurgery, and Psychiatry*, 23, 56–62.

Hinson, V. K., Cubo, E., Comella, C. L., Goetz, C. G., & Leurgans, S. (2005). Rating scale for psychogenic movement disorders: Scale development and clinimetric testing. *Movement Disorders*, 20, 1592–1597.

Inuggi, A., Sanz-Arigita, E., Gonzalez-Salinas, C., Valero-Garcia, A. V., Garcia-Santos, J. M., & Fuentes, L. J. (2014). Brain functional connectivity changes in children that differ in impulsivity temperamental trait. *Frontiers in Behavioral Neuroscience*, 8, 156.

Jenkinson, M., & Smith, S. (2001). A global optimisation method for robust affine registration of brain images. *Medical Image Analysis*, 5, 143–156.

Lancaster, J. L., Woldorff, M. G., Parsons, L. M., Liotti, M., Freitas, C. S., Rainey, L., … Fox, P. T. (2000). Automated Talairach atlas labels for functional brain mapping. *Human Brain Mapping*, 10, 120–131.

Lee, S., Ahmed, T., Lee, S., Kim, H., Choi, S., Kim, D. S., … Shin, H. S. (2011). Bidirectional modulation of fear extinction by mediodorsal thalamic firing in mice. *Nature Neuroscience*, 15, 308–314.

Lehericy, S., Tijssen, M. A., Vidailhet, M., Kaji, R., & Meunier, S. (2013). The anatomical basis of dystonia: Current view using neuroimaging. *Movement Disorders*, 28, 944–957.

Marin, R. S., Biedrzycki, R. C., & Firinciogullari, S. (1991). Reliability and validity of the apathy evaluation scale. *Psychiatry Research*, 38, 143–162.

Markovic, V., Agosta, F., Canu, E., Inuggi, A., Petrovic, I., Stankovic, I., … Filippi, M. (2017). Role of habenula and amygdala dysfunction in Parkinson disease patients with punding. *Neurology*, 88, 2207–2215.

Mehta, A. R., Rowe, J. B., & Schrag, A. E. (2013). Imaging psychogenic movement disorders. *Current Neurology and Neuroscience Reports*, 13, 402.

Mitchell, A. S. (2015). The mediodorsal thalamus as a higher order thalamic relay nucleus important for learning and decision-making. *Neuroscience and Biobehavioral Reviews*, 54, 76–88.

Neychev, V. K., Gross, R. E., Lehericy, S., Hess, E. J., & Jinnah, H. A. (2011). The functional neuroanatomy of dystonia. *Neurobiology of Disease*, 42, 185–201.

Nijenhuis, E. R., Spinhoven, P., Van Dyck, R., Van der Hart, O., & Vanderlinden, J. (1996). The development and psychometric characteristics of the Somatoform Dissociation Questionnaire (SDQ-20). *The Journal of Nervous and Mental Disease*, 184, 688–694.

O'Callaghan, C., Hornberger, M., Balsters, J. H., Halliday, G. M., Lewis, S. J., & Shine, J. M. (2016). Cerebellar atrophy in Parkinson's disease and its implication for network connectivity. *Brain*, 139, 845–855.

Perez, D. L., Barsky, A. J., Daffner, K., & Silbersweig, D. A. (2012). Motor and somatosensory conversion disorder: A functional unawareness syndrome? *The Journal of Neuropsychiatry and Clinical Neurosciences*, 24, 141–151.

Perez, D. L., Dworetzky, B. A., Dickerson, B. C., Leung, L., Cohn, R., Baslet, G., & Silbersweig, D. A. (2015). An integrative neurocircuit perspective on psychogenic nonepileptic seizures and functional movement disorders: Neural functional unawareness. *Clinical EEG and Neuroscience*, 46, 4–15.

Petrovic, I. N., Tomic, A., Voncina, M. M., Pesic, D., & Kostic, V. S. (2018). Characteristics of two distinct clinical phenotypes of functional (psychogenic) dystonia: Follow-up study. *Journal of Neurology*, 265, 82–88.

Pruim, R. H. R., Mennes, M., van Rooij, D., Llera, A., Buitelaar, J. K., & Beckmann, C. F. (2015). ICA-AROMA: A robust ICA-based strategy for removing motion artifacts from fMRI data. *NeuroImage*, 112, 267–277.

Schrag, A., Trimble, M., Quinn, N., & Bhatia, K. (2004). The syndrome of fixed dystonia: An evaluation of 103 patients. *Brain*, 127, 2360–2372.

Schrag, A. E., Mehta, A. R., Bhatia, K. P., Brown, R. J., Frackowiak, R. S., Trimble, M. R., … Rowe, J. B. (2013). The functional neuroimaging correlates of psychogenic versus organic dystonia. *Brain*, 136, 770–781.

Shakkottai, V. G., Batla, A., Bhatia, K., Dauer, W. T., Dresel, C., Niethammer, M., … Strick, P. L. (2017). Current opinions and areas of consensus on the role of the cerebellum in dystonia. *Cerebellum*, 16, 577–594.

Smith, S. M., Fox, P. T., Miller, K. L., Glahn, D. C., Fox, P. M., Mackay, C. E., … Beckmann, C. F. (2009). Correspondence of the brain's functional architecture during activation and rest. *Proceedings of the National Academy of Sciences of the United States of America*, 106, 13040–13045.

Stoodley, C. J., & Schmahmann, J. D. (2010). Evidence for topographic organization in the cerebellum of motor control versus cognitive and affective processing. *Cortex*, *46*, 831–844.

Tekin, S., & Cummings, J. L. (2002). Frontal-subcortical neuronal circuits and clinical neuropsychiatry: An update. *Journal of Psychosomatic Research*, *53*, 647–654.

Tomic, A., Agosta, F., Sarasso, E., Petrovic, I., Basaia, S., Pesic, D., … Filippi, M. (2018). Are there two different forms of functional dystonia? A multimodal brain structural MRI study. *Molecular Psychiatry* (in press). https://doi.org/10.1038/s41380-018-0222-2

Valet, M., Gundel, H., Sprenger, T., Sorg, C., Muhlau, M., Zimmer, C., … Tolle, T. R. (2009). Patients with pain disorder show gray-matter loss in pain-processing structures: A voxel-based morphometric study. *Psychosomatic Medicine*, *71*, 49–56.

Vertes, R. P., Linley, S. B., & Hoover, W. B. (2015). Limbic circuitry of the midline thalamus. *Neuroscience and Biobehavioral Reviews*, *54*, 89–107.

Voon, V., Brezing, C., Gallea, C., Ameli, R., Roelofs, K., LaFrance, W. C., Jr., & Hallett, M. (2010). Emotional stimuli and motor conversion disorder. *Brain*, *133*, 1526–1536.

Voon, V., Brezing, C., Gallea, C., & Hallett, M. (2011). Aberrant supplementary motor complex and limbic activity during motor preparation in motor conversion disorder. *Movement Disorders*, *26*, 2396–2403.

Voon, V., Gallea, C., Hattori, N., Bruno, M., Ekanayake, V., & Hallett, M. (2010). The involuntary nature of conversion disorder. *Neurology*, *74*, 223–228.

Vuilleumier, P., Chicherio, C., Assal, F., Schwartz, S., Slosman, D., & Landis, T. (2001). Functional neuroanatomical correlates of hysterical sensori-motor loss. *Brain*, *124*, 1077–1090.

Wang, H., Guo, W., Liu, F., Chen, J., Wu, R., Zhang, Z., … Zhao, J. (2016). Clinical significance of increased cerebellar default-mode network connectivity in resting-state patients with drug-naive somatization disorder. *Medicine (Baltimore)*, *95*, e4043.

Worsley, K. J., Marrett, S., Neelin, P., Vandal, A. C., Friston, K. J., & Evans, A. C. (1996). A unified statistical approach for determining significant signals in images of cerebral activation. *Human Brain Mapping*, *4*, 58–73.

SUPPORTING INFORMATION

Additional supporting information may be found online in the Supporting Information section at the end of this article.